Electronic Supplementary Material (ESI) for Nanoscale.
This journal is © The Royal Society of Chemistry 2021

Electronic Supplementary Information for:

Dimensionality-Driven Metal-Insulator Transition in Spin-Orbit-Coupled IrO_2

E. Arias-Egido,[a,b] M. A. Laguna-Marco,[a,b,c] C. Piquer,[a,b] P. Jiménez-Cavero,[a,b] I. Lucas,[a,b] L. Morellón,[a,b] F. Gallego,[d] A. Rivera-Calzada,[d] M. Cabero-Piris,[e] J. Santamaria,[d,f,g] G. Fabbris,[h] D. Haskel,[h] R. Boada,[i,j] and S. Díaz-Moreno[j]

[a] *Instituto de Nanociencia y Materiales de Aragón (INMA), CSIC - Universidad de Zaragoza, Zaragoza 50009.* [b] *Departamento de Física de la Materia Condensada, Universidad de Zaragoza, Zaragoza 50009, Spain.* [c] *Instituto de Ciencia de Materiales de Madrid, CSIC, Cantoblanco, 28049 Madrid,* [d] *GFMC, Universidad Complutense de Madrid, 28040 Madrid, Spain.* [e] *ICTS - Centro Nacional de Microscopía Electrónica, Universidad Complutense de Madrid, 28040 Madrid, Spain.* [f] *Laboratorio de Heteroestructuras con aplicación en spintrónica, Unidad Asociada UCM/CSIC, 28049 Madrid, Spain.* [g] *GFMC, Instituto de Magnetismo Aplicado, Universidad Complutense de Madrid, 28040 Madrid, Spain.* [h] *Advanced Photon Source, Argonne National Laboratory, Argonne, IL 60439, USA.* [i] *Department of Chemistry Universitat Autonoma de Barcelona 08193 Bellaterra, Barcelona, Spain.* [j] *Diamond Light Source Ltd Harwell Science and Innovation Campus Didcot,Oxfordshire OX11 0DE, UK.*

I. STRUCTURAL CHARACTERIZATION

The thickness of the thicker films ($t > 3$ nm) was calculated from the XRR data in Fig. S1. For the thinner samples ($t \leq 3$ nm) t was calculated from XRD data (in the main text).

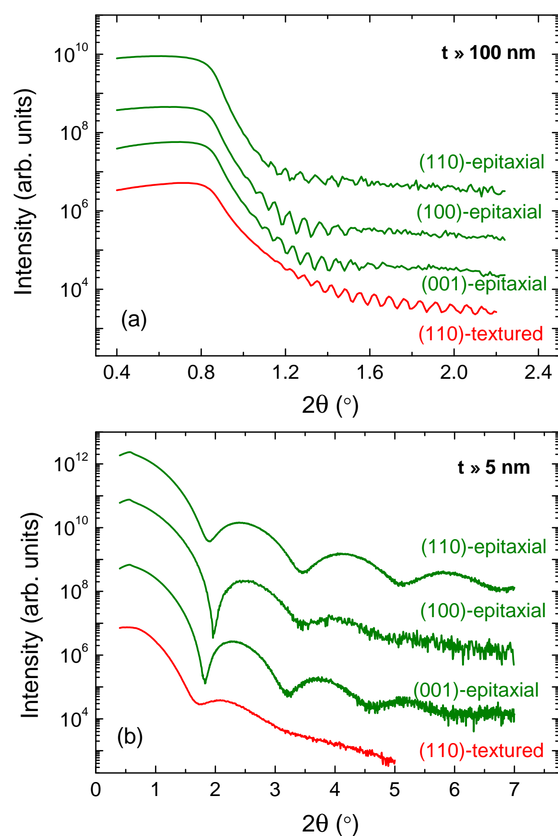

FIG. S1: XRR measurements on IrO2 thin films for nominal (a) t = 100 nm and (b) t = 5 nm.

The polycrystalline film with $t \sim 100$ nm, displays the typical XRD peaks of rutile-IrO_2, with the relative intensity of the (110)-peak clearly enhanced indicating (110) texture. Rietveld analysis of this diffractogram points to a slightly compressed lattice parameters (a = 4.49 Å and c = 3.16 Å) relative to IrO_2 polycrystallline bulk samples(a = 4.50 Å and c = 3.13 Å). Besides, the remarkable difference between the average (out-of-plane) crystallite grain size determined from XRD (GS $\sim$ 18 nm) and the GS observed in the surface SEM images (Fig. S2) confirms the platy-like shape of the grains, in agreement with a XRD *Pref.* parameter < 1.

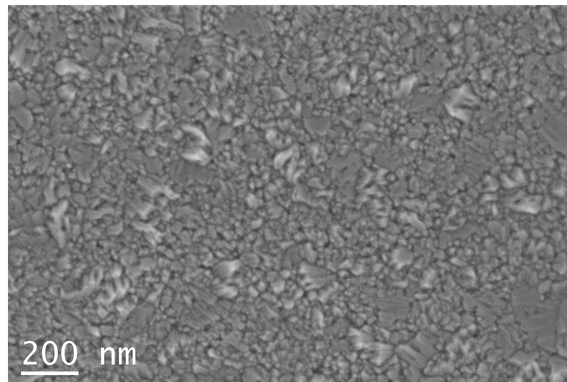

FIG. S2: Surface FE-SEM image recorded on 100 nm-thick (110)-textured film.

Thinner (110)-textured samples do not show diffraction peaks. However, the XAS spectra display well-defined features even for the thinner samples as shown in Fig. S3, which shows that the samples are not amorphous.

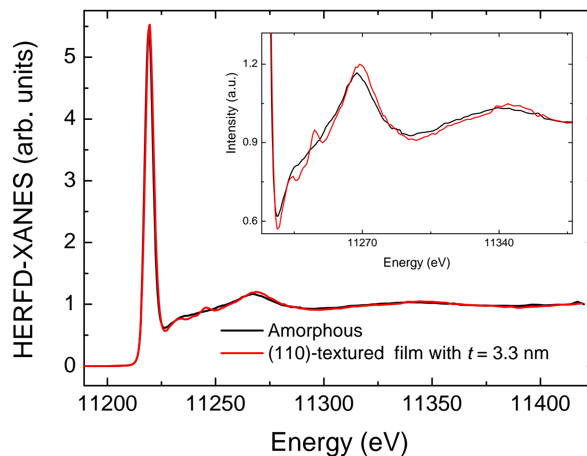

FIG. S3: Comparison of the XAS spectra recorded at the Ir L_3 edge on an amorphous 20 nm-thick film and a polycrystalline (110)-textured film with t = 3.3 nm.

Regarding the epitaxial films, lattice parameters were obtained from the reciprocal space maps (RSM) collected on 100 nm- and 5 nm-thick samples shown in Fig. S4. Different lattice parameters (different degrees of tensile/compresile strain) are obtained depending on the growth direction and thickness. Regarding the films on TiO_2 (001), in the 100 nm-thick film the extended spot shows that the in-plane lattice parameters a and b present both a gradual relaxation along the thickness, from 4.59 Å (same as in substrate) to 4.50 Å; and the out-of-plane parameter c, from 3.12 Å (greater than in substrate, 2.96 Å) to 3.15 Å. By contrast, in the t = 5 nm film the in-plane lattice parameters are perfectly matched with the substrate ($a = b$ = 4.59 Å) and the out-of-plane parameter c is compressed to compensate the tensile strain down to 3.11 Å. As for the epitaxial films on TiO_2 (100), in the 100 nm-thick film, represented in panels (e) and (f) of Fig. S4, it can be seen that the in-plane lattice parameter b, is matched with the substrate (4.59 Å), although the spot seems to be slightly extended indicating a small relaxation. The other in-plane lattice parameter c, is compressed down to 3.13Å, and hence, it does not completely match the value of the substrate (2.96 Å). The out-of-plane parameter a, is compressed down to 4.46 Å. In the t = 5 nm film the in-plane parameter b, is

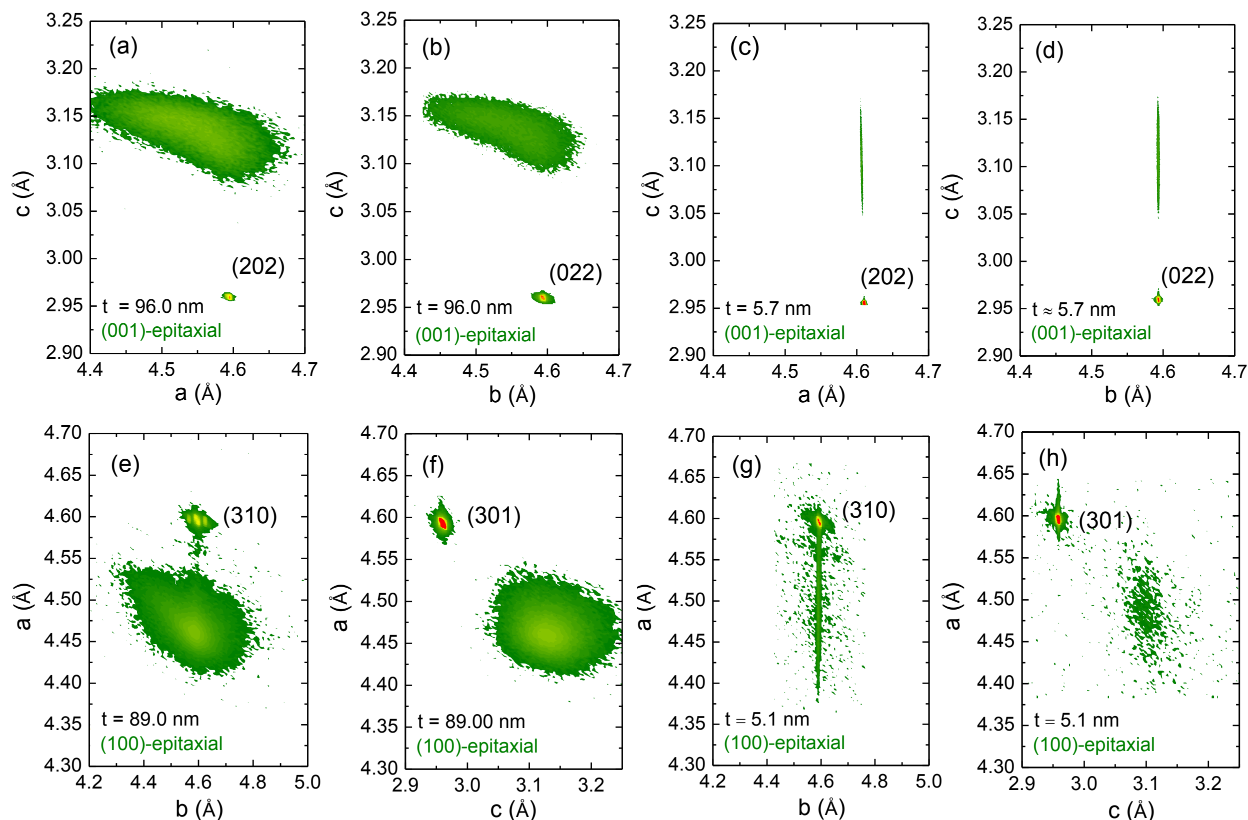

FIG. S4: Reciprocal space maps for epitaxial films deposited on TiO_2 (001) with t = 96.0 nm (a) and (b), on TiO_2 (001) with t = 5.7 nm (c) and (d), on TiO_2 (100) with t = 89.0 nm (e) and (f) and on TiO_2 (100) with t = 5.1 nm (g) and (h).

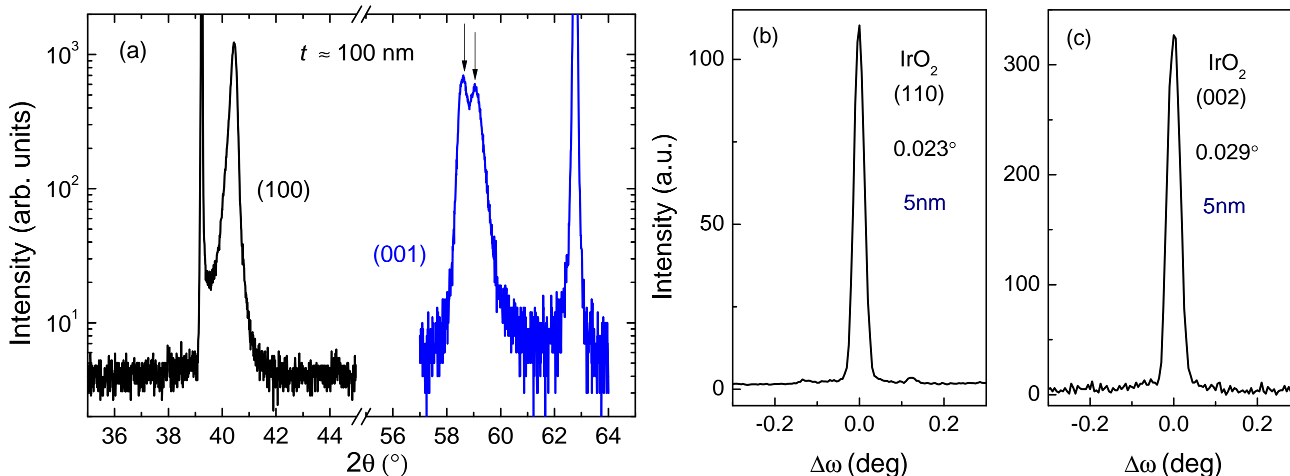

FIG. S5: (a) XRD measurements for ∼ 100 nm-thick epitaxial films deposited on TiO2(100) and TiO2(001). Rocking curves of the (110) (b) and (002) (c) peaks obtained for the 5 nm-thick films with (110) and (001) orientation, respectively.

again matched (4.59 Å, tensile strain). The other in-plane parameter, c, is more compressed down to 3.10 Å, though it is not yet fully matched with the substrate. The out-of-plane parameter, a, is compressed down to 4.48 Å.

In the XRD patterns no signs of relaxation is observed in thinner samples. By contrast, in the 100 nm-thick samples some signs of relaxation are observed in agreement with the RSMs. Hence, the double peak observed in the 100 nm-thick (001)-epitaxial sample at $2\theta = 58.5°$ and $59.0°$ (marked with arrows in Fig. S5(a)), is due to the fact

that two differentiated regions with two different lattice parameters are present in the sample instead of a gradual evolution of the lattice parameters. This is associated to the three-step fabrication process. In the 100 nm-thick (100)-epitaxial sample the asymmetric shape of the Bragg peak observed at $2\theta = 40.5°$ may be due to a strain gradient (gradual relaxation).Panels (b) and (c) of Fig. S5 show two representative rocking curves for films with $t \leq 5$ nm. The full width at half maximum found for these samples is in the 0.022°-0.032° range.

II. XANES CHARACTERIZATION

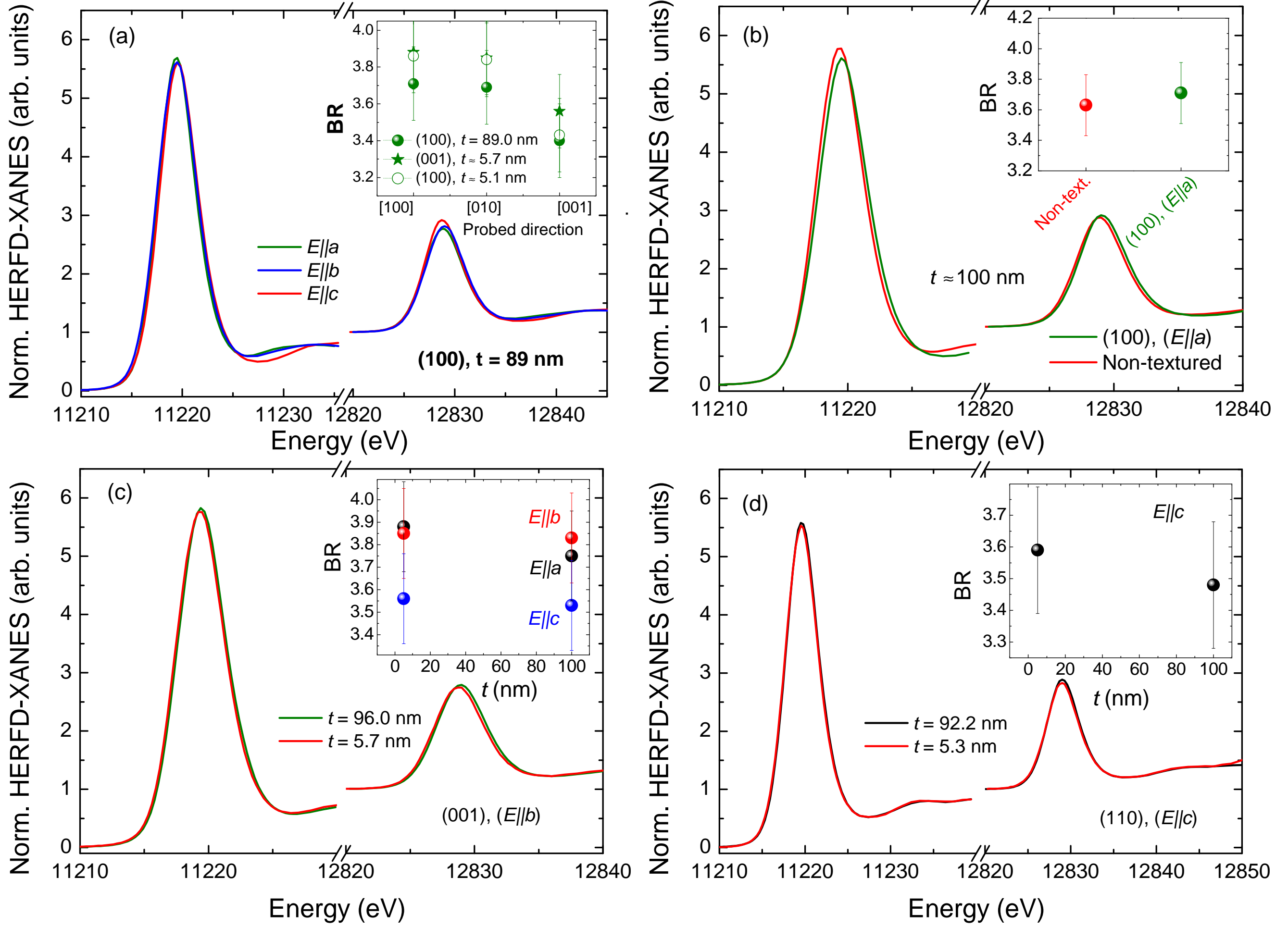

FIG. S6: Representative comparison between the normalized Ir $L_{2,3}$-edges HERFD-XANES spectra recorded (a) along different directions, (b) on an epitaxial film and a reference polycrystalline non-textured (GS = 10 nm) IrO_2 film, (c) on (001)-epitaxial samples with different t and (d) on (110)-epitaxial samples with different t. The values of the branching ratio obtained in different samples are included in the insets. In all the cases self-absorption effects were corrected using the XANDA software.[1]

As shown in Fig. S6 very similar spectral profiles can be observed in the Ir $L_{2,3}$-edge HERFD-XANES spectra recorded for all the measured samples. First of all, the lack of significant linear natural dichroism in IrO_2 should be noticed. The differences are very small when different directions are probed by varying the alignment of the crystal with respect to the incident X-ray polarization vector ($\mathbf{E}//a$, $\mathbf{E}//b$ or $\mathbf{E}//c$) (Fig. S6(a)). Only subtle yet robust differences are observed: at the L_3 edge the threshold shifts ~ 0.3 eV towards higher energy and the decrease of the absorption right after the whiteline is more pronounced when the [001] direction is probed. At the Ir L_2 edge the intensity of the whiteline increases respect to the [010] and [100] directions. Secondly, in Fig. S6(b) a representative comparison between the spectra recorded on samples with different degree of crystallinity is displayed. Little difference is observed between the polycrystalline and epitaxial films.

Similarly, only very small differences are observed in the XANES spectra as the layer thickness is reduced: a decrease

in the intensity of both whitelines and a small shift (< 0.5 eV) towards low energy are barely observable (see Fig. S6 (c) and (d)). Even when HERFD-XANES does not provide enough resolution to clearly reveal the change of the electronic structure, the t-driven shift in energy in the HERFD-XANES spectra is in agreement with that observed in angle-integrated measurements of the valence bands.[2]

TABLE I: Branching ratio (BR) calculated from the XANES spectra recorded at the Ir $L_{2,3}$ edges. For the sake of completeness the value of $\langle \mathbf{L} \cdot \mathbf{S} \rangle$ has been directly calculated for the polycrystalline non-textured reference sample as well as estimated by doing a polarization average and assuming cubic symmetry and d^5occupation (5 holes) for those epitaxial film where the three directions were measured.

Sample Orientation	*t* (nm)	Probed Direction	BR (±0.22)	⟨L·S⟩
(100)	89	[100]	3.71	1.74
		[010]	3.69	
		[001]	3.4	
	5.1	[100]	3.86	1.81
		[010]	3.84	
		[001]	3.43	
	1.7	[100]	3.92	
		[010]	4.22	
(001)	96	[100]	3.75	1.81
		[010]	3.83	
		[001]	3.53	
	5.7	[100]	3.88	1.85
		[010]	3.85	
		[001]	3.56	
(110)	92.2	[001]	3.48	
	5.3	[001]	3.59	
(110)-textured	106.5		3.64	
Non-textured	80.5		3.63	1.76

For isotropic systems the ground-state expectation value of the angular part of the spin-orbit coupling $\langle \mathbf{L} \cdot \mathbf{S} \rangle$, can be determined by applying sum rule analysis to the HERFD-XANES spectra, $BR = (2 + \langle \mathbf{L} \cdot \mathbf{S} \rangle / n_h)/(1 - \langle \mathbf{L} \cdot \mathbf{S} \rangle / n_h)$, where BR is the ratio of the integrated whiteline intensity recorded at the Ir $L_{2,3}$ edges, $BR = I_{L_3}/I_{L_2}$.[3,4]. In single crystals this relation cannot be straightforwardly applied to the polarization-dependent XAS spectra. Despite of this, some qualitative information about the evolution of the $\langle \mathbf{L} \cdot \mathbf{S} \rangle$ with thickness can still be obtained. In all the cases the BR slightly increases as t decreases, provided that the same direction is probed (see table I). The slight enhancement observed in BR may be indicative of an increase of $\langle \mathbf{L} \cdot \mathbf{S} \rangle$ as a result of enhanced localization in the thinnest samples. By reducing the layer thickness the coordination of constituent ions at the interfaces is reduced. This may yield a decrease of both, the orbital overlap and W,[5] thus increasing the effective SOC. In fact, recent angle-resolved photoemission spectroscopy (ARPES) studies have reported narrower W in ultrathin IrO_2 films[6].

III. RESISTIVITY

TABLE II: Resistivity and residual resistivity ratio of IrO_2 epitaxial films with $t \geq 5$ nm.

film orientation	t (nm)	ϱ @ 10 K ($\mu\Omega$ cm)	RRR
001	96.0	31	2.0
001	5.7	47	1.9
100	89.0	40	2.0
100	5.1	95	1.5
110	92.2	55	1.6
110	5.3	193	1.3

For the ∼2-3 nm-thick films a slope change, from dρ/dT>0 at high T to dρ/dT<0 at low T, is observed at T_{min}.

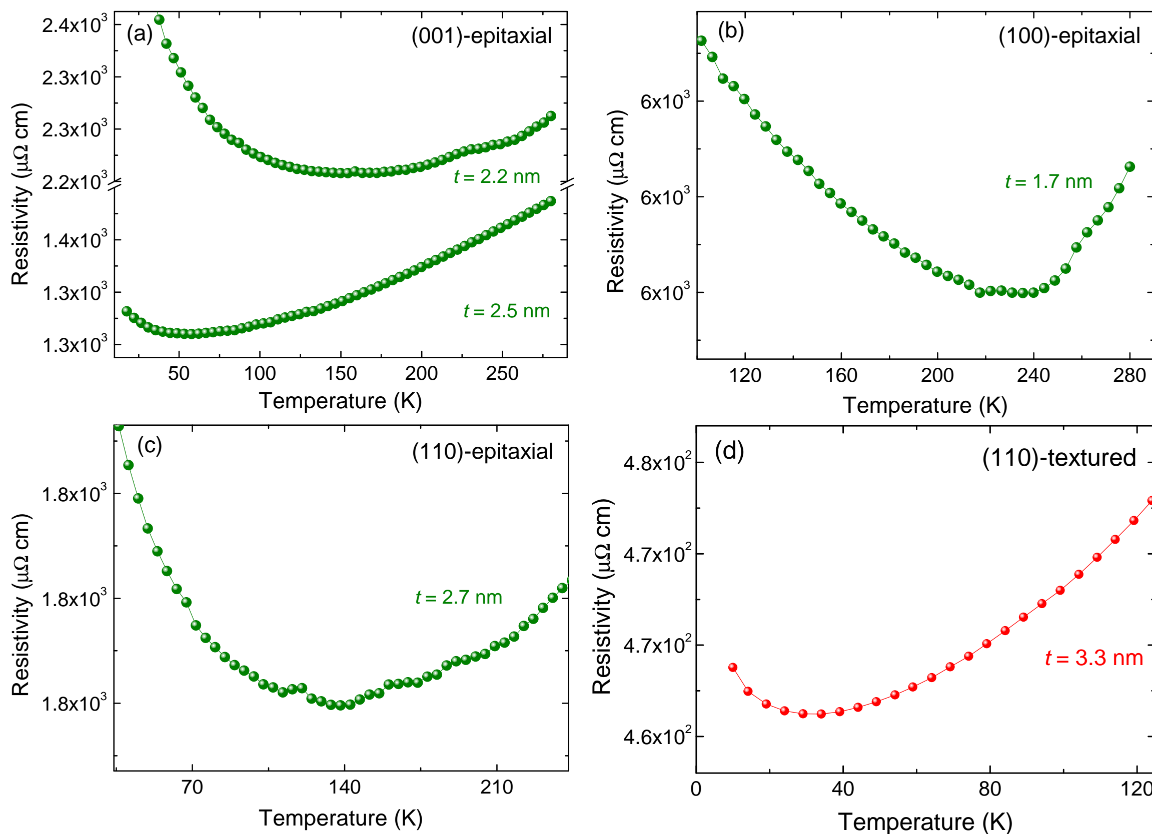

FIG. S7: Detail of the upturns in the ρ(T) curves for (a) (001)-epitaxial, (b) (100)-epitaxial, (c) (110)-epitaxial and (d) (110)-textured samples with different thickness.

---

[1] K. V. Klementiev, XANES dactyloscope for Windows, freeware: https://intranet.cells.es/Beamlines/CLAESS/software/xanda.html.

[2] J. K. Kawasaki, D. Baek, H. Paik, H. P. Nair, L. F. Kourkoutis, D. G. Schlom, and K. M. Shen, Phys. Rev. Materials **2**, 054206 (2018).

[3] G. van der Laan and B. T. Thole, Phys. Rev. Lett. **60**, 1977 (1988).

[4] M. A. Laguna-Marco, D. Haskel, N. Souza-Neto, J. C. Lang, V. V. Krishnamurthy, S. Chikara, G. Cao, and M. van Veenendaal, Phys. Rev. Lett. **105**, 216407 (2010).

[5] D. E. McNally, X. Lu, J. Pelliciari, S. Beck, M. Dantz, M. Naamneh, T. Shang, M. Medarde, C. W. Schneider, V. N. Strocov, et al., npj Quant. Mater. **4**, 6 (2019).

[6] J. K. Kawasaki, C. H. Kim, J. N. Nelson, S. Crisp, C. J. Zollner, E. Biegenwald, J. T. Heron, C. J. Fennie, D. G. Schlom, and K. M. Shen, Phys. Rev. Lett. **121**, 176802 (2018).